



***Trigonella foenum-graecum* down-regulated Osteopontin, TNF- α , and IL-12 and up-regulated IL-10 in Paracetamol induced Nephrotoxicity in rats**

Amal Attia El-Morsy Ibrahim^{1,2} and Turki M. Al-Shaikh²

¹Department of Zoology, Faculty of Girls' for Arts, Education and Science, Ain Shams University, Cairo, Egypt.

²Department of Biological Sciences, Faculty of Science, Northern Border University, KSA.

Corresponding author: Amal Attia El-Morsy Ibrahim. amal_ai_elmorsy@yahoo.com

ABSTRACT

The using of pain relief is increases day by day, and many people especially youth are used to consume overdoses from these drug to kill pain. From these drugs and the most famous is paracetamol. Paracetamol (PAR) overdose (750 mg/kg) can cause nephrotoxicity with oxidative stress as one of the possible mechanisms mediating the event. The present study aimed to examine the effects of Trigonella foenum-graecum (200 mg/kg) on PAR-induced nephrotoxicity, for seven consecutive days. Treatment with Trigonella (TRIGO) prevented the PAR-induced nephrotoxicity. The nephron-protective effects of Trigonella were confirmed by a reduced intensity of renal cellular damage, as evidenced by histological findings. Decreased serum levels of TNF- α , IL-12, total protein, albumin and decrease expression of proliferating cell nuclear antigen (PCNA) and osteopontin renal tissue when compared with PAR-treated animals. TRIGO enhanced and increased serum levels of IL-10. In conclusion, TRIGO has a protective role against PAR-induced nephrotoxicity by reducing inflammatory activity.

Keywords: *Trigonella – paracetamol – kidney – TNF- α – IL-2 – IL-10*

Received 22.06.2016

Revised 26.07.2016

Accepted 11.08.2016

INTRODUCTION

Kidneys play a major role in the metabolism and excretion of drugs, making it susceptible to various drug induced damage. Paracetamol (PAR) is a worldwide household analgesic-antipyretic drug virtually devoid of typical anti-inflammatory activity and hence free of some of the side-effects of aspirin and related agents, e.g. gastric erosion and bleeding complications [1]. PAR accidental or intentional overdose causes acute liver and kidney failure [2,3]. Because of its clinical importance PAR-induced acute toxicity has become an essential model for studying drug induced liver and kidney injury. At therapeutic doses, PAR is metabolized via glucuronidation and sulfuration reactions occurring primarily in the liver, and results in water-soluble metabolites that are excreted via the kidney. It is known that the incidence of nephrotoxicity is less common than that of hepatotoxicity as delineated by Blakely & McDonald [4]. PAR administration documented the induction of renal tubular damage and acute renal failure can occur even in the absence of liver damage [5,6], and can be the primary manifestation of PAR toxicity [2].

Plant drugs are frequently considered to be less toxic and freer from side-effects than synthetic ones [7]. Fenugreek or *Trigonella foenum-graecum* (TRIGO), a perennial herb; of the Leguminosae family. It is widely distributed in Egypt, India, Greece, Lebanon, Spain, Italy, France and Turkey. It is a well-known traditional medicinal herb, and possesses pharmacological functions. TRIGO seeds have been used as traditional medicines not only in diabetes [8] but also in high cholesterol, inflammation and gastrointestinal ailments [9]. Fenugreek seeds contain lysine and L-tryptophan rich proteins, mucilaginous fibre, coumarin, fenugreekine, nicotinic acid, phytic acid, scopoletin and trigonelline, and other rare chemical constituents such as saponins. Saponins are a large group which composed of diosgenin, yamogenin, gitogenin, tigogenin, sapogenins, and neotigogens, which are thought to account for many of its significant therapeutic effects [10,11].

As PAR overdose is shown to mediate severe renal damage, which can be life-threatening, treatments that could offer maximum protection against PAR are therefore needed. The present study, aimed to

determine the potential protective effects of TRIGO against PAR-induced nephrotoxicity. The effects were determined by investigation of the histopathological changes, expression of osteopontin and PCNA in the renal tissue; and expression of TNF- α , IL-12, and IL-10 in serum.

MATERIALS AND METHODS

Drug sources

Paracetamol tablets (500 mg) were purchased from Glaxo Smith Kline (GSK) Company, United Kingdom. Trigonella tablets (610 mg) were purchased from General Nutrition Corporation (GNC), USA.

Experimental protocol

Twenty-eight male *Rattus rattus* rats (110 \pm 10 g) were obtained from the Egyptian Organization for Vaccine and Biological Preparations in Helwan, Egypt. The animals were housed in solid plastic cages with a wire mesh lid, 4 rats/rectangular cage. They were housed in a controlled environment with room temperature and a 12 h light/dark cycle. Animals were fed mouse pellet and fresh water *ad libitum* for a week prior to experiments. Rats were randomly divided into four groups containing 7 animals each and all treatments were given daily for seven days. PAR and TRIGO were administered orally. Rats in Group I served as the control group and were administered distilled water only. Groups II received 200 mg/kg TRIGO, according to Chaturvedi *et al.* [12]. Group III received 750 mg/kg PAR, according to Sathishkumar & Baskar [13]. In Group IV, rats were treated with 750 mg/kg PAR and 200 mg/kg of TRIGO. On Day 8, all animals were anaesthetized with sodium phenobarbital to minimize suffering and then scarified. All animal procedures are in accordance with the recommendations of the Canadian committee for care and use of animals (Canadian Council on Animal Care [CCAC], [14]).

Measurement of kidney function and protein profile

Blood samples were collected in sterile centrifuge tubes. Serum was separated after leaving the blood to clot and then centrifuged at 3000 rpm for 10 min. Serum samples were kept in clean, dry and sterile glass vials for kidneys function determination. Urea was determined according to the method of Patton and Crouch [15], creatinine was determined following the method of Young *et al.* [16], and uric acid was determined by the method of Schirmeister *et al.* [17]. Total protein was determined according to the method of Peters [18] and albumin was determined by the method of Doumas and Giggs [19].

Cytokines Activity

Cytokine activities of TNF- α , IL-10, and IL-12 in serum were measured via a highly sensitive commercial ELISA (Sandwich Immunoassay Technique) specific kit for rats. Briefly, 96-well microplates were coated with TNF- α (R&D System, #45418, Minneapolis, MN, USA), IL-10 (R&D System #67232, Minneapolis, MN, USA), and IL-12 (ThermoFisher Scientific, #KRC0121, www.thermofisher.com) antibodies and incubated overnight at room temperature. The plates were washed with PBS containing 0.05% Tween 20 and then blocked with PBS with 1% bovine serum albumin and 5% sucrose. After the addition of diluted samples and standard TNF- α , IL-10, and IL-12 dilutions, plates were incubated for 2h at room temperature. Biotinylated goat anti-rat was used as the detection antibody, and streptavidin-HRP was added as the conjugate to each well. Equal proportions of hydrogen peroxide and tetramethylbenzidine were used as the substrate solution, and the reaction was stopped by adding 2N sulfuric acid. All samples and standards were run in duplicate, and the optical density was determined with a microplate reader at a wavelength of 450nm. The values of plasma cytokine concentration were expressed as pm/ml.

Histopathological investigations

Examination of renal histology was performed according to routine histology techniques. After the animal was sacrificed, the kidney was rinsed with normal saline, and sectioned into small pieces. The specimens were then fixed in 10% formalin, dehydrated in stepwise with ascending concentration of ethanol solution (70% to 100%), and embedded in paraffin. Using a microtome, tissue sections of 4 μ m thickness were produced, fixed overnight on the slide, subsequently stained with hematoxylin and eosin (H-E), and observed under a light microscope [20].

Immunohistochemical studies

The expression of osteopontin (ab63856, Abcam), and proliferating cell nuclear antigen (PCNA) (ab2426, Abcam, Cambridge Science Park in Cambridge, England) in kidney sections was determined immunohistochemically in formalin-fixed, paraffin-embedded tissue. Blocks were cut into 4 mm thick sections mounted on glass slides, and incubated at 4°C overnight. Sections were deparaffinized in xylene and rehydrated. Endogenous peroxidase activity was blocked with 1% hydrogen peroxide for 20 min. To improve the quality of staining, microwave oven-based antigen retrieval was performed. Slides were probed with either anti-osteopontin (1:100, rabbit mAb, 5 μ g/ml, for 15 min at room temperature), or anti-PCNA (1:500, rabbit mAb). Sections were washed 3 times with PBS for 10 min each and incubated with biotin-labeled anti-mouse IgG for 1 h at room temperature. After washing, sections were stained

with a streptavidin-peroxidase detection system according to the manufactured instructions. Positive control slides showed no staining when the primary antibody was omitted.

Counting PCNA-Positive Nuclei

Five sections of each experimental group were randomly selected. Five fields were randomly selected from each slide where ~ 400 nuclei were counted [21]. Every stained nucleus was considered positive, regardless of intensity. The percentage of positive stained cells were recorded as the PCNA labeling index (LI). Positive and negative cells were counted and the labeling index percentage of cells immunostained for PCNA (PCNA-LI(%)) was calculated using the following equation: PCNA-LI (%) = (+nuclei/ total nuclei)*100.

Where: +nuclei are the no. of PCNA positive staining nuclei and total nuclei are the sum of the immunostained and non-immunostained within the same field.

Statistical analysis

Statistical analysis was done using SPSS version (16). Data were analyzed using one way analysis of variance (ANOVA) was used for comparison between groups followed by post-hoc Duncan test. Data were expressed as mean±standard error (SE) and P<0.05 showed statistically significance.

RESULTS

Kidney function analysis

Table (1) showed the effect of TRIGO serum urea and creatinine concentrations in PAR-induced nephrotoxic rats for 7 days. PAR-induced significant (p<0.05) elevations in the serum concentrations of urea and creatinine. These elevations were significantly (p<0.05, p<0.01, p<0.001) inhibited in TRIGO treated rats. PAR administration caused depletion in total protein and albumin serum levels which reversed as a result of TRIGO administration; returning near to the normal values.

Table (1): Biochemical analysis of kidney function and protein profile in control and experimental groups.

Groups	C	TRIGO	PAR	PAR+TRIGO
Urea (mg/dl)	18.29 ± 0.38	18.24 ± 0.67 ^{cd}	53.04 ± 1.71 ^{abd}	38.45 ± 1.33 ^{abc}
Creatinine (mg/dl)	0.70 ± 0.033	0.70 ± 0.031 ^c	2.10 ± 0.28 ^{abd}	1.01 ± 0.14 ^c
Uric acid (mg/dl)	2.79 ± 0.39	2.68 ± 0.39 ^{cd}	7.83 ± 0.51 ^{abd}	4.89 ± 0.33 ^{abc}
Total protein (g/dl)	8.20 ± 0.49	9.31 ± 0.51 ^c	3.80 ± 0.42 ^{abd}	7.68 ± 0.69 ^c
Albumin (g/dl)	4.87 ± 0.43	5.41 ± 0.35 ^{cd}	2.29 ± 0.28 ^{abd}	3.36 ± 0.23 ^{abc}

Values are mean±SE. Superscript letters denote the significance at (p<0.05); a: Significant to C, b: significance to TRIGO, c: Significant to PAR, and d: significant to PAR+TRIGO

Detection of the cytokines TNF-α, IL-10, and IL-12 by ELISA, revealed that PAR administration elevated the concentrations of TNF-α and IL-12; while decrease in IL-10 levels relative to control group, reached 23.45, 29.81 and 23.88 pg/ml respectively as recorded in table 2. This elevation in TNF-α and IL-12 is an obvious evident for renal inflammation. TRIGO treatment counteracted PAR side effect on pro-inflammatory cytokine production where these levels recorded 12.09, 10.77 and 28.39 pg/ml for TNF-α, IL-12, and IL-10 respectively. These results suggested the protective effect of TRIGO in preventing renal damages.

Table (2): IL-1β, IL-6 and TNF-α cytokines levels in control and experimental groups (pg/ml)

Groups	C	TRIGO	PAR	PAR+TRIGO
TNF-α	5.11 ± 0.37	4.55 ± 0.41 ^{cd}	23.45 ± 1.43 ^{abd}	12.09 ± 0.86 ^{abc}
IL-12	6.75 ± 0.30	6.70 ± 0.47 ^{cd}	29.81 ± 0.35 ^{abd}	10.77 ± 0.32 ^{abc}
IL-10	37.40 ± 0.67	37.69 ± 0.64 ^{cd}	23.88 ± 1.73 ^{ab}	28.39 ± 0.66 ^{abc}

Values are mean±SE. Superscript letters denote the significance at (p<0.05); a: Significant to C, b: significance to TRIGO, c: Significant to PAR, and d: significant to PAR+TRIGO

Histological investigation

Renal sections from the control and TRIGO groups showed no histological changes, as evidenced by the normal appearance of glomeruli and tubules (Figs. 1 & 2). Kidney sections delineated normal architecture of the renal tissue appeared in the preserved renal parenchyma, rounded glomeruli, proximal convoluted tubules with narrow lumen lined by cuboidal epithelium and distal convoluted tubules with wide lumen in the renal cortex (Fig. 1). Renal tissue from rats treated with 200 mg/kg TRIGO showed no histopathological changes when compared with control animals (Fig. 2).

The effects of PAR on nephritis damage were evaluated by the extensive disruption of tissue architecture; destruction of the normal pattern of the renal tissue; enlarged glomeruli with widened Bowman's capsule. Sections from kidney from rats administered PAR revealed distorted glomerulus that containing RBCs in its cavity, renal tubule cavities filled with hyaline cast and cellular debris (Fig. 3); segmented glomeruli

with widened Bowman's space, tubulointerstitial nephritis and the renal tubules appeared with pyknotic nuclei, beside the presence of lymphocytic infiltrations (Fig. 4); and destruction of the renal tubules with disintegrated tubular cells with pyknotic nuclei, distension of Bowman's space as appeared in the figure (5).

Despite the short duration of treatment with TRIGO, but it proved its protective effect in improving the renal architecture. Lesions that appeared as a result of PAR administration were remarkably reduced in the renal tissue sections of the TRIGO treated rats. Kidney sections revealed apparent normal renal parenchyma, but still glomeruli appeared with slight segmentaion. The proximal convoluted tubules appeared near to normal with their narrow lumen (Fig. 6).

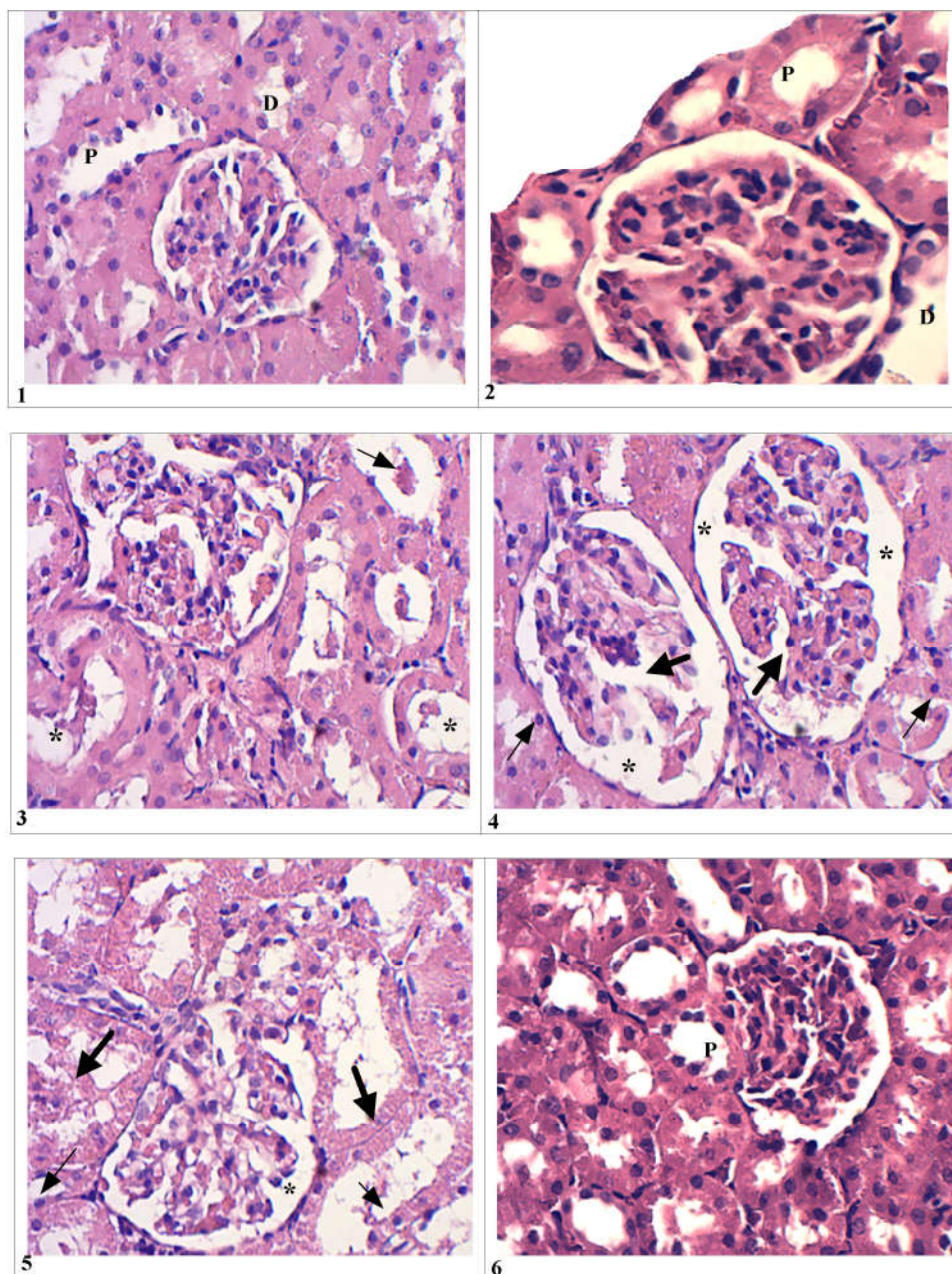


Fig. 1: Photomicrograph of the renal cortex from control rat, showing the normal histological structure of renal parenchyma, rounded glomeruli, distal convoluted tubules with wide lumen (D) and proximal (P) convoluted tubules with narrow lumen lined by cuboidal epithelium. (H-E, X 400).

Fig. 2: Photomicrograph of the renal medulla from control rat showing proximal convoluted tubules (P) with narrow lumen lined by cuboidal epithelium and distal convoluted tubules (D) with wide lumen in the renal cortex. (H-E, X 400).

Fig. 3: Photomicrograph of the renal cortex, from rat treated with PAR showing distorted glomerulus that containing RBCs in its cavity, renal tubule cavities filled with cellular debris (*) and hyaline cast (arrow). (H-E, X400).

Fig. 4: Photomicrograph of the kidney section from rat administered with PAR, showing segmented glomeruli (thick arrows) with widened Bowman's space (*), tubulointerstitial nephritis and the renal tubules appeared with pyknotic nuclei (thin arrows), beside the presence of lymphocytic infiltrations (head arrow). (H-E, X 400).

Fig. 5: Photomicrograph of the renal cortex, from rat administered with PAR, showing destruction of the renal tubules with disintegrated tubular cells (thick arrows) with pyknotic nuclei (thin arrows), distension of Bowman's space (*) (H-E, X 400).

Fig. 6: Photomicrograph of the renal cortex, from rat treated with TRIGO showing apparent normal renal parenchyma, but still glomeruli appeared with slight segmentaion. The proximal convoluted tubules appeared near to normal with their narrow lumen (P). (H-E, X 400).

Immunohistochemical investigations

Osteopontin expression

Kidney cross sections from control rats stained immunohistochemically for osteopontin delineated osteopontin positive cells distributed only in the cytoplasm of renal tubules (Fig. 7). Sections from TRIGO treated rats showed no expression of osteopontin neither in the renal tubules or in the glomeruli (Fig. 8). On the other hand, kidney section from rats received PAR, revealed an increase in osteopontin expression in the cytoplasm of renal tubules, refer to the tubulointerstitial nephritis (Fig. 9). Kidney sections of rats treated with PAR+TRIGO showed decreased osteopontin expression (Fig. 10), when compared with PAR group.

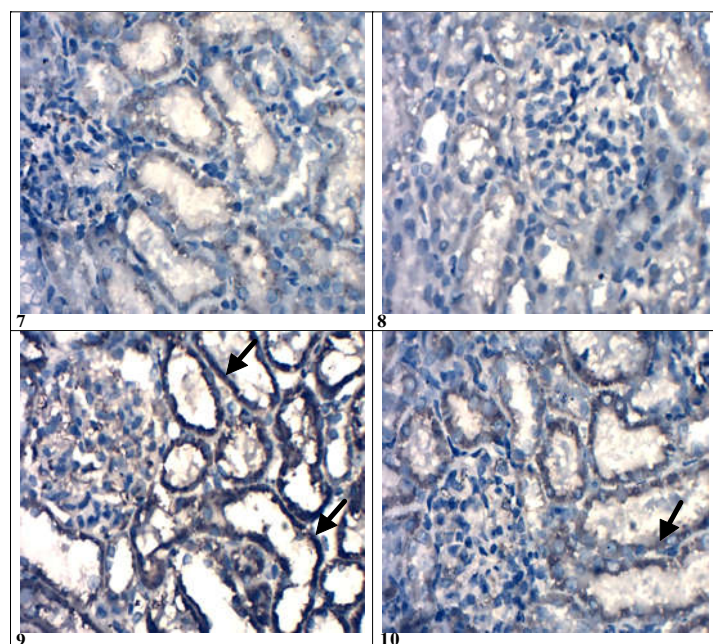


Fig. (7): Photomicrograph of kidney section from control rat showing osteopontin distributed in the cytoplasm of some cells of renal tubules, and positive staining in the glomerulus (Immunohistochemical stain, X400).

Fig. (8): Kidney section from rat treated with TRIGO showing no osteopontin expression in the renal tubules or the glomerulus (Immunohistochemical stain, X400).

Fig. (9): Kidney section from rat treated with PAR showing increased expression of osteopontin intense staining in brown in kidney tubules (arrow) (Immunohistochemical stain, X400).

Fig. (10): Kidney section from rat treated with PAR+TRIGO showing decrease in osteopontin (arrow) distribution as compared with PAR treated rat (Immunohistochemical stain, X400).

Proliferating cell nuclear antigen (PCNA) expression

Cross sections of kidney from control and TRIGO treated rats stained immunohistochemically for PCNA delineated no PCNA positive cells distributed in the glomeruli; while +ve PCNA nuclei are showed in the renal tubules (Figures 11&12). On the other hand, kidney section from rats received PAR, revealed an increased PCNA +cells in renal tubules, as a result of nephritis (Fig. 13). TRIGO administration caused a decrease in PCNA +cells in renal tubules (Fig. 14).

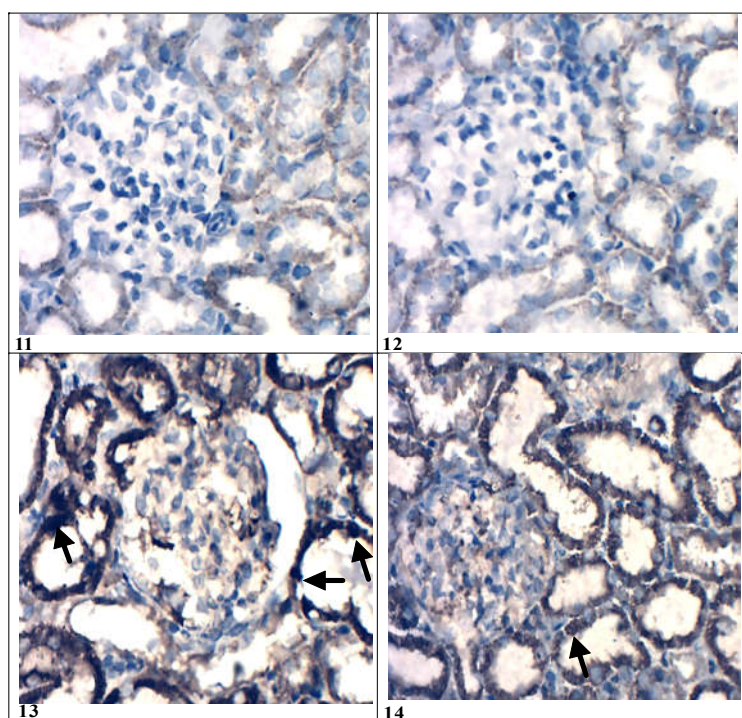


Fig. (11): Photomicrographs of kidney section from control rat showing the normal expression of PCNA (arrow) in the renal tubules, while glomeruli showing negative staining (Immunohistochemical stain, X400).

Fig. (12): Kidney section from rat treated with TRIGO showing slight expression of PCNA in the renal tubules, and negative staining in glomeruli (Immunohistochemical stain, X400).

Fig. (13): Kidney section from treated with PAR showing renal tubules with increase expression of PCNA+ve nuclei staining in brown in (arrow) (Immunohistochemical stain, X400).

Fig. (14): Kidney section treated with PAR+TRIGO showing decrease in PCNA+ nuclei expression (arrow) as compared with PAR treated rat (Immunohistochemical stain, X400).

The increased apoptotic activity of renal tissue cells reported in PAR treated rats, reached 19.11% as compared with control (7.14%) and TRIGO treated rats (6.03%). Decrease in PCNA-LI recorded (11.97%) in the renal tissue from PAR+TRIGO as shown in table (3) when compared with PAR treated group.

Table 3: Averages of PCNA-LI (%) in control and different experimental groups

Groups	C	TRIGO	PAR	PAR+TRIGO
Mean (+ve nuecli ~400 nuclei)	28.56 ± 1.18	24.12 ± 0.78 ^{acd}	76.44 ± 2.15 ^{abd}	47.88 ± 1.09 ^{abc}
PCNA-LI (%)	7.14	6.03	19.11	11.97

Values are mean±SE. Superscript letters denote the significance at (p<0.05); a: Significant to C, b: significance to TRIGO, c: Significant to PAR, and d: significant to PAR+TRIGO

DISCUSSION

PAR toxicity is one of the major causes of poisoning worldwide [22], and its overdose is commonly associated with hepatic [23] and renal damages [24]. PAR administration significantly (p < 0.05) increased TNF-α and IL-12 expressions compared to control and TRIGO administered groups. PAR+TRIGO administration normalized the increase in TNF-α and IL-12 expressions that are observed in PAR administered group. Moreover, TRIGO administration plus PAR significantly increased the expression of regenerative IL-10. IL-12 was identified as a disulfide-linked heterodimeric cytokine composed of 35 and 40 Ku subunits. IL-12 secreted principally by antigen presenting cells (APC), such as macrophages, B cells, and dendritic cells, activates natural killer (NK) cells and T cells to produce interferon-γ (IFN-γ), and augments their cytotoxic activity and proliferation [25]. TNF-α, is a pro-inflammatory cytokine produced by macrophages/monocytes during acute inflammation and leading to necrosis or apoptosis [26]. Diosgenin (DG) a component of TRIGO; restore the antioxidants status in renal tissues in rats with renal failure [27]. DG inhibited TNF-α induced production of intracellular reactive oxygen species (ROS) and phosphorylation of mitogen activated protein kinases (MAPK) as reported by Choi *et al.* [28] and Ibrahim [11]. Moreover, the present results agree with Fouad *et al.* [29] and Ahmad *et al.* [30] indicated that increased production of TNF-α in renal tissue that indicates the pathogenesis of PAR-induced nephrotoxicity. On the other hand, IL-10 is a major anti-inflammatory cytokine that has diverse effects on both innate and adaptive immunity [31]. IL-10 can inhibit the synthesis of pro-

inflammatory cytokines such as IFN- γ and TNF- α produced by cells such as M ϕ and regulatory T-cells [32]. The decrease in TNF- α and IL-12 levels and the increase in IL-10 Levels in the present study revealed the anti-inflammatory effect of TRIGO.

Osteopontin, a glycoprotein with a glycine-arginine-glycine-aspartate-serine (GRGDS) cell binding domain, has been described in bone and is also known to be expressed in other organs, particularly the kidney [33]. Multiple studies have demonstrated that osteopontin is expressed by inflammatory cells such as macrophages and highly induced during inflammatory activation [34]. Osteopontin appears to be constitutively expressed but in all cells studied it is rapidly upregulated following cellular activation by a variety of growth factors and cytokines (including NO, Ang II, IL-1 β , IFN- γ , TNF- α , TGF β) as reported by Gao *et al.* [35]. Polarization of Th cells to the Th1 or Th2 phenotypes, a critical aspect of cell-mediated immunity, is influenced by osteopontin which enhances Th1 and inhibits Th2 cytokine expression [36]. Osteopontin induces macrophages to express IL-12 and stimulates T-cells to express INF- γ and CD40 ligand, which subsequently induces IL-12 expression from monocytes [37]. Thus, osteopontin provides an important early stimulus for IL-12 production at sites of inflammation. Osteopontin further inhibits IL-10 expression by macrophages and thereby decreases anti-inflammatory signaling pathways [38]. Collectively, the present study supported the anti-inflammatory effect of TRIGO in spite of its administration for a short period.

A 36-kDa DNA auxiliary protein; known as PCNA, which accumulates in the nucleus during S phase of the cell cycle. It plays a crucial role in the cellular DNA synthesis, in DNA nucleotide excision-repair, and nucleic acid metabolism [39]. TRIGO had a suppressor effect on the expression of PCNA +cells which revealed its protective role in inflammatory conditions.

The biochemical and the histopathological investigations are in harmony with the cytokine study. PAR-induced acute renal damage is induced by the elevations in blood urea, creatinine and uric acid levels and occurrence of tubulointerstitial nephritis as appeared histologically [40,41]. The kidney is thought to form a toxic metabolite only when it is glutathione depleted. The animals studied indicated that when the kidney is overwhelmed with PAR, its oxidation via the P-450 system results in tubular damage [40,42]. Previous studies have shown that the elevation of renal MDA levels can be attributed in part to NAPQI which is the reactive metabolite product caused by PAR induced nephrotoxicity, leads to GSH depletion and covalently binds to cysteine residues on proteins, which results in lipid peroxidation reaction [43]. Increased level of NAPQI mediates oxidative damage, interact with the cellular macromolecules; and finally enhancing the cellular injuries and renal dysfunction [44]. Manimaran *et al.* [44] stated that PAR reduced GSH by 60–90%, indicating inefficient detoxification of NAPQI. Treatment with PAR caused a statistically significant decrease in renal SOD activities. Reduction in the activity of SOD is likely to be a result of futile cycling of P450, caused by NAPQI which utilized reducing equivalent of NADPH with concomitant reduction of molecular superoxide anion radical (O $_2^{\cdot-}$), hence there will be a reduction in superoxide dismutase activity [45]. Therefore, an overdose of PAR will saturate the conjugation pathways of GSH and cause depletion of cellular GSH; reducing its capacity to detoxify NAPQI.

da silva Melo *et al.* [46] detected the renal acute lesions at 24 h after PAR (650 mg/kg) administration by urinalysis. The study stated higher levels of urinary epithelial cells, γ -glutamyltransferase (GGT), alkaline phosphatase (ALP) and lactate dehydrogenase (LDH) enzymes. While, Neto *et al.* [1] showed that PAR at a dose level of 500 or 1,500 mg/kg, during pregnancy revealed kidney degeneration and necrotic foci, and mitochondrial cytolysis in the convoluted tubules in both maternal and fetal tissues.

Although the period of treatment with TRIGO is short (7 days), renal architecture showed many improvements if compared with PAR-induced renal toxicity. TRIGO with its components of bioactive phytochemicals normalized the kidney function and the histological picture of renal tissue by its antioxidant and anti-inflammatory activities [12].

Conclusion

The present data concluded that Trigo confers protection against functional and histopathological injuries in the kidneys of PAR treated rats by improving kidney function, increasing activities of antioxidants and restoring the histological picture of the kidney. Therefore, the present study suggesting an alternative treatment for PAR toxicity; by using a natural source for the protection; as a potent mediator of cellular immunity.

REFERENCES

1. Neto, J.A., Oliveira-Filho, R.M., Simões, M.J., Soares, J.M. Jr. & Kulay, L. Jr. (2004). Long-term acetaminophen (paracetamol) treatment causes liver and kidney ultra-structural changes during rat pregnancy. Clin. Exp. Obst. Gynecol. 31(3):221-4.
2. Boutis, K. & Shannon, M. (2001). Nephrotoxicity after acute severe acetaminophen poisoning in adolescents. J. Toxicol. Clin. Toxicol. 39: 441–445.

3. Larson, A.M., Polson, J., Fontana, R.J., Davern, T.J., Lalani, E., Hynan, L.S., Reisch, J.S., Schiodt, F.V., Ostapowicz, G., Shakil, A.O. & Lee, W.M. (2005). Acetaminophen-induced acute liver failure: results of a United States multicenter, prospective study. *Hepatology*. 42: 1364–1372.
4. Blakely, P. & McDonald, B.R. (1995). Acute renal failure due to acetaminophen ingestion: a case report and review of the literature. *J. Am. Soc. Nephrol.* 6:48–53.
5. Carpenter, H.M. & Mudge, G.H. (1981). Acetaminophen nephrotoxicity: studies on renal acetylation and deacetylation. *J. Pharmacol. Ex. Ther.*, 218: 161–167
6. Abdul Hamid, Z., Budin, S.B., Jie, N.W., Hamid, A., Husain, K. & Mohamed, J. (2012). Nephroprotective effects of *Zingiber zerumbet* Smith ethyl acetate extract against paracetamol-induced nephrotoxicity and oxidative stress in rats. *J Zhejiang University Science B-(Biomed & Biotech)*. 13(3):176–185.
7. Altan, N. & Kilic, N. (1997). Effect of the sulfonylurea glyburide on superoxide dismutase in streptozotocin-induced diabetic rat muscle. *General Pharmacol.* 28: 795–796.
8. Mowla, A., Alauddin, M., Rahman, A. & Ahmed, K. (2009). Antihyperglycemic effect of *Trigonella foenum-graecum* (fenugreek) seed extract in alloxan-induced diabetic rats and its use in diabetes mellitus: a brief qualitative phytochemical and acute toxicity test on the extract. *Af. J. Trad. Complemen. Alter. Med.* 6(3): 255–261
9. Sharma, R.D., Raghuraman, T.C. & Rao, N.S. (1990). Effect of fenugreek on blood glucose and serum lipids in type I diabetes. *Eur. J. Clin. Nutr.* 44(4):301–306.
10. Billaud, C. & Adrian, J. (2001). Fenugreek: Composition, nutritional value and physiological properties. *Sciences-des-aliments*, 21: 3–26.
11. Ibrahim, A.A.E. (2015). Mechanism of Action of *Trigonella* in Cancer Prevention. *Am. J. Bio. Life Sci.* 3(2): 43–49.
12. Chaturvedi, U., Shrivastava, A., Bhaduria, S., Saxena, J.K. & Bhatia, G. (2013). A mechanism-based pharmacological evaluation of efficacy of *Trigonella foenum graecum* (fenugreek) seeds in regulation of dyslipidemia and oxidative stress in hyperlipidemic rats. *J. Cardiovasc. Pharmacol.* 61(6):505–12.
13. Sathishkumar, T. & Baskar, R. (2014). Renoprotective effect of *Tabernaemontana heyneana* Wall. leaves against paracetamol-induced renotoxicity in rats and detection of polyphenols by high-performance liquid chromatography–diode array detector–mass spectrometry analysis. *J. Acute Med.* 4(2):57–67.
14. Candian Council on Animal Care (CCAC). (1993). Guide to the Care and Use of Experimental Animals. CCAC, Ottawa, Ontario, Canada. Vol.1: pp.1–298
15. Patton, C.J. & Crouch, S.R. (1977). Spectrophotometric and kinetics investigation of the Berthelot reaction for the determination of ammonia. *Anal. Chem.* 49:464–469.
16. Young, D.S., Pestamer, L.C. & Gibber-Man, V. (1975). Effect of drugs on clinical laboratory tests. *Clin. Chem.* 21(5):1D–432D.
17. Schirmeister, J., Willmann, H. & Kiefer, H. (1964). Plasma kreatinin als grober Indikator der Nierenfunktion. *Deutsche medizinische Wochenschrift*. 89:1018.
18. Peters, T. (1968). Determination of total proteins. *Clin. Chem.* 14:1147–1159.
19. Doumas, B.T. & Giggs, H.G. (1971). Albumin standard and measurement of serum albumin with bromocresol green. *Clin. Chim. Acta.* 31:78
20. Bancroft, J.D. & Gamble, M. (2002). Theory and practice of histological techniques. 5th ed. London: Churchill Livingstone.
21. Ibrahim, A.A.E. (2013). Does fennel has a protective effect against cigarette smoke exposure in rat pulmonary and testicular tissues? Does consumption of *Pimpinella anisum* associated with testicular damage? *J. Toxicol. Health.* 103 (2013): 266–292.
22. Gunnell, D., Murray, V. & Hawton, K. (2000). Use of paracetamol (acetaminophen) for suicide and non-fatal poisoning: world-wide patterns of use and misuse. *Suicide Life Threat. Behav.* 30:313–20.
23. Nelson, S.D. (1995). Mechanisms of the formation and disposition of reactive metabolites that can cause acute liver injury. *Drug Metab. Rev.* 27: 147–177.
24. Placke, M.E., Wyand, D.S. & Cohen, S.D. (1987). Extrahepatic lesions induced by acetaminophen in the mouse. *Toxicol. Pathol.*, 15,381–383
25. Gately, M.K., Renzetti, L.M., Magram, J., Stern, A.S., Adorini, L., Gubler, U. & Presky, D.H. (1998). The interleukin-12/interleukin-12-receptor system: role in normal and pathologic immune responses. *Annu. Rev. Immunol.* 16:495–521.
26. Idriss, H.T. & Naismith, J.H. (2000). TNF alpha and the TNF receptor superfamily: structure-function relationship(s). *Microscopy Res. Tech.* 50(3):184–95.
27. Manivannan, J., Barathkumar, T.R., Sivasubramanian, J. Arunagiri, P., Raja, B., & Balamurugan, E. (2013). Diosgenin attenuates vascular calcification in chronic renal failure rats. *Mol. Cell. Biochem.* 378(1–2):9–18. doi:10.1007/s11010-013-1588-8
28. Choi, K.W., Park, H.J., Jung, D.H., Kim, T.W., Park, Y.M., Kim, B.O., Sohn, E.H., Moon, E.Y., Um, S.H., Rhee, D.K. & Pyo, S. (2010). Inhibition of TNF- α -induced adhesion molecule expression by diosgenin in mouse vascular smooth muscle cells via downregulation of the MAPK, Akt and NF- κ B signaling pathways. *Vasc. Pharmacol.* 53:273–280.
29. Fouad, A.A., Qureshi, H.A., Yacoubi, M.T. & Al-Melhim, W.N. (2009). Protective role of carnosine in mice with cadmium-induced acute hepatotoxicity. *Food Chem. Toxicol.* 47:2863–2870
30. Ahmad, S.T., Arjumand, W., Nafees, S., Seth, A., Ali, N., Rashid, S. & Sultana, S. (2012). Hesperidin alleviates acetaminophen induced toxicity in wistar rats by abrogation of oxidative stress, apoptosis and inflammation. *Toxicol. Letters*. 208: 149– 161 .

31. Wang, S., Gao, X., Shen, G., Wang, W., Li, J., Zhao, J., Wei, Y-Q. & Edwards, C.K. (2016). Interleukin-10 deficiency impairs regulatory T cell-derived neuropilin-1 functions and promotes Th1 and Th17 immunity. *Sci. Rep.* 6:1-16. Article number:24249
32. Donnelly, R.P., Freeman, S.L. & Hayes, M.P. (1995). Inhibition of IL-10 expression by IFN-gamma up-regulates transcription of TNF-alpha in human monocytes. *J. Immunol.* 155: 1420-1427.
33. Brown, L.F., Berse, B., Van de Water, L., Papadopoulos-Sergiou, A., Perruzzi, C.A., Manseau, E.J., Dvorak, H.F. & Senger, D.R. (1992). Expression and Distribution of Osteopontin in Human Tissues: Widespread Association with Luminal Epithelial Surfaces. *Molec. Bio. Cell.* 3: 1169-1180.
34. Lund, S.A., Wilson, C.L., Raines, E.W., Tang, J., Giachelli, C.M. & Scatena, M. (2013). Osteopontin mediates macrophage chemotaxis via alpha4 and alpha9 integrins and survival via the alpha4 integrin. *J. Cell. Biochem.* 114:1194-1202.
35. Gao, C., Guo, H., Mi, Z., Wai, P.Y. & Kuo, P.C. (2005). Transcriptional regulatory functions of heterogeneous nuclear ribonucleoprotein-U and -A/B in endotoxin-mediated macrophage expression of osteopontin. *J. Immunol.* 175:523-530.
36. Ashkar, S., Weber, G.F., Panoutsakopoulou, V., Sanchirico, M.E., Jansson, M. & Zawaideh, S. (2000). Eta-1 (osteopontin): an early component of type-1 (cell-mediated) immunity. *Sci.* 287:860-864.
37. O'Regan, A.W., Hayden, J.M. & Berman, J.S. (2000). Osteopontin augments CD3-mediated interferon- γ and CD40 ligand expression by T cells, which results in IL-12 production from peripheral blood mononuclear cells. *J. Leukocyte Biol.* 68:495-502.
38. Bruemmer, D., Collins, A.R., Noh, G., Wang, W., Territo, M. & Arias-Magallona, S. (2003). Angiotensin II-accelerated atherosclerosis and aneurysm formation is attenuated in osteopontin-deficient mice. *J. Clin. Invest.* 112:1318-1331.
39. Levine, E., Cupp, A.S., Miyashiro, L. & Skinner, M.K. (2000). Role of transforming growth factor- α and the epidermal growth factor receptor in embryonic rat testis development. *Biol. Reprod.* 62:477-490.
40. Abraham, P. (2005). Oxidative stress in paracetamol-induced pathogenesis: (1)- Renal Damage. *Ind. J. Biochem. Biophys.* 42:59-62
41. Singh, D.P. & Mani, D. (2015). Protective effect of *Triphala Rasayana* against paracetamol-induced hepato-renal toxicity in mice. *J. Ayurv. Integ. Med.* 6(3): 181-186.
42. Mitic-Zlatkovic, M., Cukuranovic, R. & Stefanovic, V. (1998). Urinary enzymes excretion after acute administration of paracetamol in patients with kidney disease. *Scient J FACTA UNIVERSITATIS: Med. Biol.* 5(1):40-43.
43. Dahlin, D.C., Miwa, G.T., Lu, A.Y. & Nelson, S.D. (1984). N-acetyl-p-benzoquinone imine: a cytochrome P-450-mediated oxidation product of acetaminophen. *Proc. Nat. Acad. Sci. USA.* 81(5):1327-31
44. Manimaran, A., Sarkar, S.N. & Sankar, P. (2010). Influence of repeated preexposure to arsenic on acetaminophen-induced oxidative stress in liver of male rats. *Food Chem. Toxicol.* 48: 605-610.
45. Sharma, S., Chaturvedi, J., Chaudhari, B.P., Singh, R.L. & Kakkar, P. (2012). Probiotic *Enterococcus lactis* ITRHR1 protects against acetaminophen-induced Hepatotoxicity. *Nutr.* 28: 173-181.
46. da Silva Melo, D.A., Saciura, V.C., Poloni, J.A., Oliveira, C.S., Filho, J.C., Padilha, R.Z., Reichel, C.L., Neto, E.J., Oliveira, R.M., D'avila, L.C., Kessler, A. & de Oliveira, J.R. (2006). Evaluation of renal enzymuria and cellular excretion as a marker of acute nephrotoxicity due to an overdose of paracetamol in Wistar rats. *Clin. Chim. Acta.* 373 (1-2): 88-91.

CITATION OF THIS ARTICLE

Amal Attia El-Morsy Ibrahim and Turki M. Al-Shaikh. *Trigonella foenum-graecum* down-regulated Osteopontin, TNF- α , and IL-12 and up-regulated IL-10 in Paracetamol induced Nephrotoxicity in rats. *Bull. Env. Pharmacol. Life Sci.*, Vol 5 [10] September 2016: 05-13